Electric and magnetic signatures of dust devils from the 2000–2001 MATADOR desert tests

W. M. Farrell,[1] P. H. Smith,[2] G. T. Delory,[3] G. B. Hillard,[4] J. R. Marshall,[5] D. Catling,[6] M. Hecht,[7] D. M. Tratt,[7,8] N. Renno,[9] M. D. Desch,[1] S. A. Cummer,[10] J. G. Houser,[1] and B. Johnson[4]

[1]   Dust devils are significant meteorological phenomena on Mars: They are ubiquitous, continually gardening the Martian surface, and may be the primary atmospheric dust-loading mechanism in nonstorm seasons. Further, dust grains in the swirling dust devils may become electrically charged via triboelectric effects. Electrical effects associated with terrestrial dust devils have been reported previously, but these were isolated measurements (electric fields only) with no corroborating measurements. To study the fluid and electrical forces associated with dust devils, NASA's Human Exploration and Development of Space (HEDS) enterprise sponsored a set of desert field tests with a suite of mutually compatible and complementary instruments in order to determine the relationship between electric, magnetic, and fluid forces. The project (originally a selected flight project) was entitled "Martian ATmosphere And Dust in the Optical and Radio" (MATADOR). In this work, we present a number of interesting examples of the electromagnetic nature of the dust devil. We also describe potential hazards of the dust devil and how similar devil- and storm-related forces on Mars might affect any human occupation.   *INDEX TERMS:* 6225 Planetology: Solar System Objects: Mars; 3304 Meteorology and Atmospheric Dynamics: Atmospheric electricity; 3379 Meteorology and Atmospheric Dynamics: Turbulence; 3394 Meteorology and Atmospheric Dynamics: Instruments and techniques; 0305 Atmospheric Composition and Structure: Aerosols and particles (0345, 4801); *KEYWORDS:* triboelectricity, electric fields, dust devils, magnetic fields, atmospheric electricity

1. Motivation

[2]   The atmosphere of Mars is very arid, windy [*Ryan and Lucich*, 1983], and of very low pressure (1% of the terrestrial atmosphere). Entrained in the Martian surface winds is dust in both saltation and suspension. As the dust grains come in contact with the surface and with each other, they will exchange charge via triboelectric (frictional) processes [*Eden and Vonnegut*, 1973]. Tribo-electricity (tribo has a Greek origin meaning "to rub") is also referred to as contact electrification. The associated charge exchange is a quantum effect resulting from bringing the Fermi energy of two originally isolated grains to the same energy level upon contact [*Ashcroft and Mermin*, 1976]. This tribocharging process is anticipated to be particularly strong on Mars: The very low atmospheric pressure will allow grains to also draw charge from the atmosphere, and arid climate guarantees that atmospheric water molecules will not scavenge charge from the grains.

[3]   Tribocharging effects are expected to be strongest when dust is saltated into large concentrations driven by atmospheric instabilities (i.e., dust devils and dust storms). On Earth, there are isolated measurements of dust devil electrical properties. It has been found that dust devils of $\sim$10 meters width and $\sim$100–200 meters height can develop very large DC electric fields exceeding several hundred volts/meter [*Freier*, 1960; *Crozier*, 1964]. The charge concentration in these dust devils is $\sim$10^6 e/cm^3, and is comparable to the charge concentration of the terrestrial ionosphere. On Mars, such dust devils and storms are larger than those on Earth (they measure from kilometers to global scales). Given the more favorable atmosphere for grains to create and hold charge, electric effects are anticipated to be prevalent on Mars, but as yet

[1]NASA Goddard Space Flight Center, Greenbelt, Maryland, USA.
[2]Lunar and Planetary Laboratory, University of Arizona, Tucson, Arizona, USA.
[3]Space Science Laboratory, University of California, Berkeley, California, USA.
[4]NASA Glenn Research Center, Cleveland, Ohio, USA.
[5]SETI Institute, Mountain View, California, USA.
[6]Department of Atmospheric Sciences, University of Washington, Seattle, Washington, USA.
[7]Jet Propulsion Laboratory, Pasadena, California, USA.
[8]NASA Earth Science Technology Office, Greenbelt, Maryland, USA.
[9]Atmospheric, Oceanic and Space Sciences, University of Michigan, Ann Arbor, Michigan, USA.
[10]Department of Computer and Electrical Engineering, Duke University, Durham, North Carolina, USA.

have not been quantified directly via surface electricity packages.

[4] MATADOR is a combined atmospheric electricity, meteorology, and imaging package comprising both in situ and remote sensing instruments specifically designed to study Martian dust devils. NASA/HEDS is very interested in dust devils as a possible nuisance or hazard to future human explorers. The electrical dust devils may give rise to increased discharging and arcing in the low pressure Martian atmosphere, increased dust adhesion to space suites and equipment, and RF communication disruptions. The MATADOR instrument suite was designed to quantify these effects in situ and was selected to fly as one of four HEDS instrument contributions to the Mars Surveyor Program Mars03 Mission. However, given the losses of Mars Polar Lander and Mars Climate Orbiter, the Mars mission line was re-architected and Mars Surveyor 03 was pushed to a late-decade launch date. MATADOR consequently lost its manifest.

[5] As part of the development effort for the MATADOR package, desert field tests were performed in regions where dust devils are prevalent. The objectives of these tests were to verify the capability of the hardware and to understand the fluid and electrical nature of the "dust devil," with a view toward understanding their Martian analogs. In this paper, we describe the results from two field studies, one small test in 2000 and a second test with a more complete suite of instruments in 2001. Given the suite of instruments, we attempt to obtain a combined electric and fluid picture of the dust devils. While this approach has raised more questions than answers regarding dust devil dynamics, we show fundamentally new results indicating an intimate relationship between their electric and fluid natures.

2. Martian Atmospheric Dust

[6] Atmospheric dust is lifted from the Martian surface by episodes of eolian entrainment (eolian: Carried by the wind). However, the physics of this lifting is still not fully understood. Wind tunnel experiments [*Greeley et al.*, 1980, 1981] indicate that sand-sized particles of 100 μm in diameter are most easily moved via shear stress from horizontal winds. Smaller particles resist movement either because they are aerodynamically smooth [*Bagnold*, 1941] and/or because they develop inter-particle forces (possibly electrical in nature) [*Iversen*, 1976]. However, the size of grains in suspension are <10 μm, which is inconsistent with 100 μm ideal shear-stress lifting size.

[7] *Greeley et al.* [1992] suggested that horizontal winds initially lift the larger sand-sized particles, but once airborne they return to the surface and impart kinetic energy to smaller lighter particles. These smaller particles then get raised into suspension via the imparted momentum. Such a grain-surface impact process might also create electrical grain charging [*Jayaratne*, 1991].

[8] However, a second process that lifts smaller grains is vertical pressure gradients like those associated with hot-cored dust devils [*Ryan and Lucich*, 1993] and convective dusty hurricanes [*Gierasch and Goody*, 1973; *Gierasch*, 1974]. In this latter case, shear stress is not the lifting mechanism. Instead light grains are drawn vertically by

rising air driven by an atmospheric convective instability reacting to the inversion of a warm air mass below a cooler mass [*Renno et al.*, 1998].

[9] Dust devils are of particular interest. Analysis of the Mars Pathfinder (MPF) images found substantial atmospheric dust loading even though the major dust storm season had ceased [*Smith and Lemmon*, 1999]. The ubiquitous dust devil was cited as the primary loading mechanism during nonstorm season. MGS MOC images reveal the presence of ever-changing dust devil tracks over the entire Martian surface, further confirming their ubiquitous nature. Figure 1 shows a dust devil as viewed from the MOC camera, along with its track (labeled as "dark streak"). It is believed that the first few centimeters of soil are lifted by the dust devil, revealing the darker subsurface soil. As evident in this figure and many others, "gardening" tracks appear subtly throughout the image.

[10] Dust devils are a result of convective instability over dry regions as surfaces begin to warm [*Renno et al.*, 1998]. Specifically, just after the major dust storm season, increased sunlight reaches the planet surface. The planet reradiates this sunlight in the IR, which is readily absorbed by atmospheric water vapor and CO_2, thereby warming the near-surface. The resulting temperature-inverted air mass is unstable. The instability is manifested by the dust devil, which essentially represents a local nonlinear fluid transfer of warm low altitude air upward and cool high altitude air downward. In the process, light grains are also transported from the surface upward with the warm air mass.

[11] One important element in convective-driven dust storm systems is mass stratification: Given the same vertical fluid force, lighter grains are lifted to higher altitudes than heavier grains. An illustrative example is found in Figure 3 of *Gierasch* [1974], indicating that grains sizes of 10–100 μm remain close to the surface while grains <10 μm percolate toward the top of dusty hurricanes. As we discuss below, mass stratification is a primary process for creating a macroscopic electric dipole moment in a dust storm. We demonstrate that the fluid properties of terrestrial dust devils mirror the fluid properties of their Martian counterpart [*Ryan and Lucich*, 1983], including the presence of forces that are capable of lifting and stratifying grains.

3. Evidence for Martian Dust Electrification

[12] Mixing grains in Martian dust storms are expected to become triboelectrified. To date, there has never been a direct measurement of electrical activity from Martian dust devils or storms, primarily because the hardware required to obtain such measurements (i.e., electrostatic field sensor or radio) has not been placed on the surface. MATADOR was specifically designed to make these measurements. However, there is a substantial body of circumstantial evidence indicating that electrical effects occur.

[13] 1. Laboratory experiments. *Eden and Vonnegut* [1973] found that mixing dust grains in a chamber under Martian-like pressure can become highly electrified, generating and maintaining a charge of 10^4 el/grain. The electri-
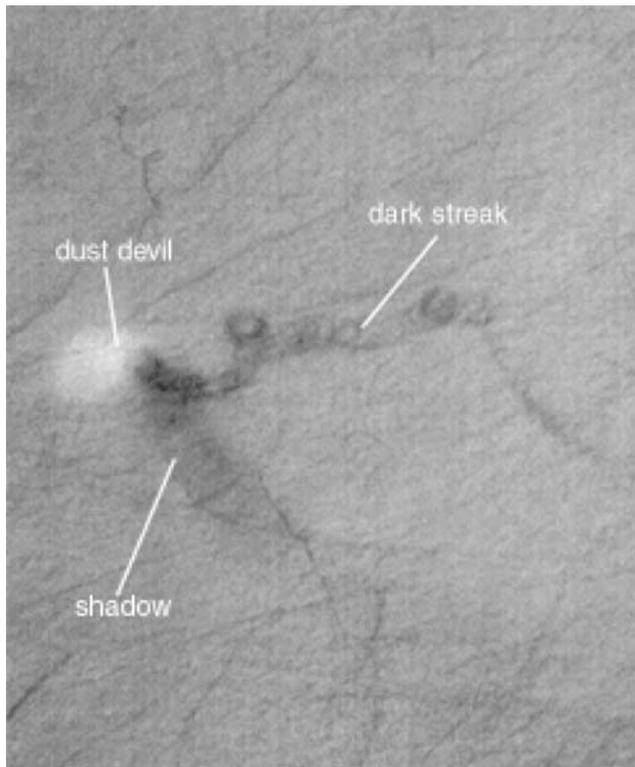
Figure 1. A MGS/MOC image of a dust devil (from M. C. Malin et al., MOC2-220, NASA's Planetary Photojournal http://photojournal.jpl.nasa.gov/, 11 December 1999).

fication was strong enough to induce glow and filamentary discharge in the low-pressure background gas. Performing a similar experiment, *Mills* [1977] was so impressed by the electrified glow of the dusty gas that he suggested charged dust could act to cleanse or scour the surface of biogenic material. *Marshall* [1994] found that electrical forces dominate grain dynamics when fluid and gravitational forces are removed (i.e., the USML-1 & -2 space shuttle experiments). *Ette* [1971] concluded that mixing, collisional dust grains will charge with a preference for smaller grains becoming negative and larger grains positive. Similarly, *Jayaratne* [1991] found that grains bouncing off an icy surface would become negatively charged, leaving the larger surface positively charged. These latter two studies suggest that the saltation layer near the surface (<1m) is electrically active.

[14] 2. Computer simulation. *Melnik and Parrot* [1998] simulated the electrical evolution of a Martian dust cloud using a two-dimensional electrostatic particle-in-cell code. This code also incorporated fluid and gravitational forces on the grains. The charge exchange between grains was based upon size [*Ette*, 1971], with the lighter grain in the collision obtaining a net negative charge in proportion to its radius. On the basis of this tribocharging scheme and vertical mass stratification due to upward winds, a substantial charge separation was found in the simulated dust storms, with light, negative charges convected to the cloud tops and heavy, positive grains to the cloud bottom. *Melnik and Parrot's* [1998] Plate 1 clearly demonstrates the influence of mass stratification on the development of the macroscopic electric field. As heavy grains descend, the lighter (-) grains

remain suspended creating a large inter-devil potential on the order of hundreds of kilovolts, with associated electric fields reaching the Martian atmospheric breakdown potential of 20 kV/m. Because of mass stratification of the charged dust, the dust cloud then obtained a macroscopic electric dipole moment (M = 2Qh, Q being the charge of each pole and h the cloud height) oriented in the nadir (downward) direction [*Farrell et al.*, 1999]. This simulation was one of the first efforts that explained the large-scale electric field development as resulting from combined fluid forces/mass stratification and a mass-preferential grain charging process.

[15] 3. Terrestrial analogs. Terrestrial dust devils provide some of the strongest indirect evidence for Martian dust devil electrification. *Freier* [1960] and *Crozier* [1964] found that modest terrestrial dust devils of ~10-m diameter and ~100-m height possess a substantial DC electric field on the order of 0.6 kV/m. These fields were consistent with the cloud possessing a macroscopic electric dipole moment, M, on the order of ~1 C-m oriented toward the nadir. This downward-directed macroscopic electric moment is consistent with smaller, negatively charged grains at the dust devil top, as simulated by *Melnik and Parrot* [1998].

[16] On the basis of this body of evidence, a general axiom has evolved: Where there are winds and mixing dust, there is triboelectricity. In essence, wind, dust and electricity are systemic processes. We expect this axiom to hold true at Mars as well, and modern Martian meteorology packages like MATADOR now include devices to quantify the electric forces generated by the windy, dusty atmosphere.

[17] *Melnik and Parrot's* [1998] simulations indicate that three processes are required for the development of a large-scale electric dipole moment in their simulated Martian dust devil: 1) Mixing grains, 2) contact electrical processes that have a mass dependency, and 3) vertical winds and gravitational field that give rise to grain mass stratification. These processes are not unique to Mars, and terrestrial dust devils should also develop large-scale quasi-electrostatic fields (as observed by *Freier* [1960] and *Crozier* [1964]) via the same three processes. Our desert observations presented here add further confirming evidence.

[18] From the discussion above, it is evident that the electric dust devil can be represented by the illustration in Figure 2. Specifically, the mass preference for grain tribo-charging along with mass stratification via upward convective winds lead to an overall charge separation in the dust devil and the development of an overall electric dipole moment. The moment-related electricity can be sensed in three different ways: First, the large scale electric field associated with the dust devil can be detected by quasi-DC E-field sensing systems such as field mills [*Freier*, 1960; *Crozier*, 1964]. Second, any change to that moment at either the macroscopic or microscopic level represents a dM/dt that gives rise to radiation [*Farrell et al.*, 1999] that can be detected as radio waves. The exact frequency of radiation depends upon the scale size and temporal nature of the currents [*Farrell et al.*, 1999]. Finally, the charged dust devil should induce potentials on objects that are immersed in the dust storm. Thus electrometers located on objects should show activity with the passage of the structure. While the DC E-fields have been reported, the second and third types of

THE ELECTRIC DUST DEVIL

- Triboelectric interactions: Lighter grains (-) charged, Heavy Grains (+) charged [Ette, 1971]

- Light Grains blown upward in convective process - charge separation

- Create Electric Dipole Moment, M, and Dipolar Electric field

- Swirling grains =Change in Moment (dM/dt)

- Terrestrial Devils we see:
    DC E-fields from M
    Radio emission from dM/dt
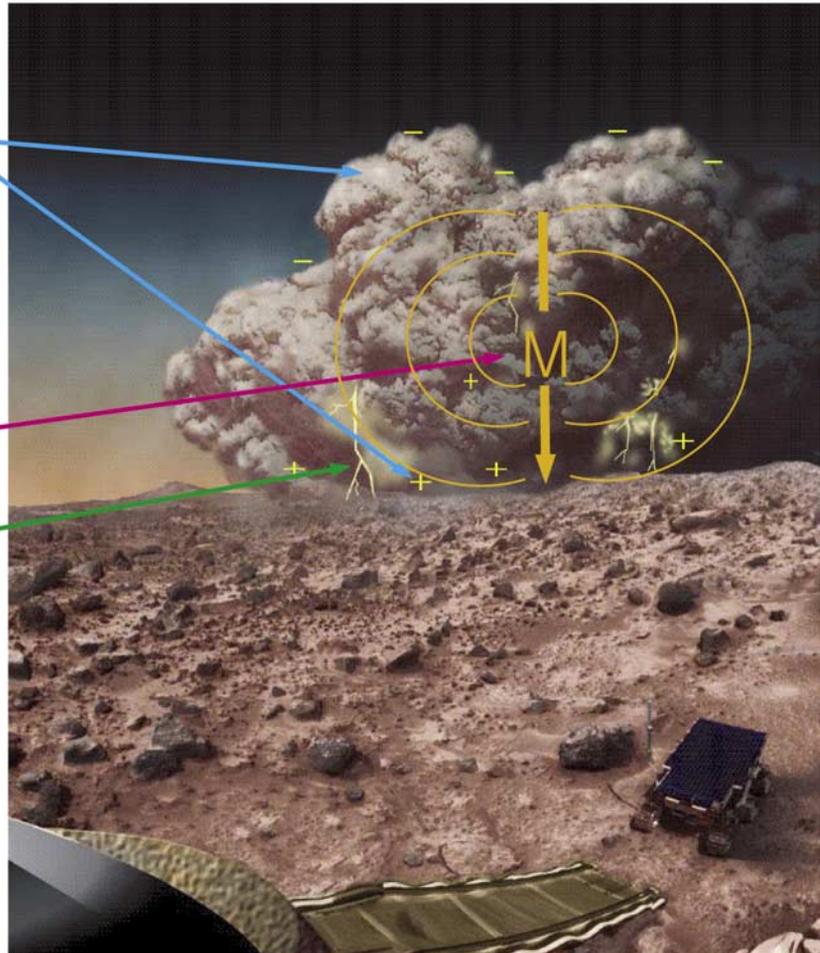   Induced Potentials on Surfaces

Figure 2. An illustration of the Electric Dust Devil.

manifestations have not been previously observed from terrestrial dust devils. We will report on observations of all three manifestations in the following discussions.
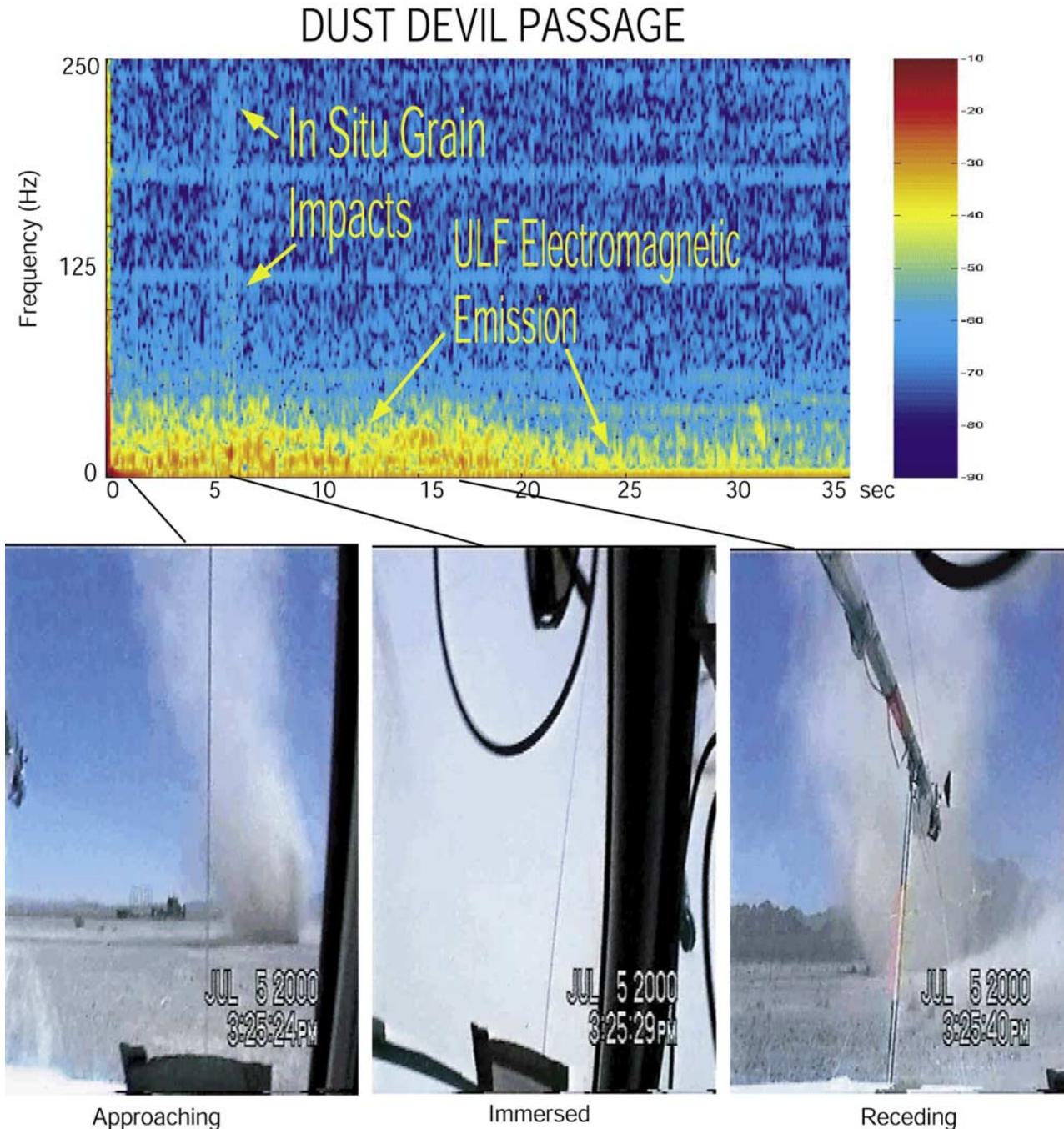
4. MATADOR Field Tests

4.1. Nevada 2000

[19] A preliminary desert test occurred in July 2000 in a Nevada playa located outside of Boulder City. *Houser et al.* [2003] have presented initial observations from this study. The primary instruments involved were a VCR camcorder and an ELF magnetic search coil antenna (i.e., low frequency magnetic radio). Signals from the latter were fed directly into the audio track of the VCR camcorder. This analog data collection process allowed the magnetic waveform signals and imaging data to be simultaneously collected and stored on dual parallel tracks. The dust devils were observed and tracked via a specially outfitted truck with an extension boom for immersion into the structured. The magnetic antenna was on this boom while the camera was located in the truck cab.

[20] The developmental state of the dust devils varied but in one particular case the truck approached and intercepted a relatively large mature dust devil (∼10m wide, 100–200 meters tall) that was clearly churning and uplifting ("gardening") sand and dust from the surface.

[21] Figure 3 shows the dust devil approach, immersion, and recession from the truck. As described previously [*Houser et al.*, 2003], two magnetic signatures were detected during this period (which are labeled in the figure). First, when the truck was immersed in the dust devil, electrostatic discharges occurred between the charged grains and exposed conductive portions of the sensor, resulting in a set of broadband "spiky" emissions in the data set. The broadband noise associated with this discharge is clearly evident in the spectrogram as the structure passed over the sensors, this activity appearing as vertical bands in the spectrogram.

[22] A second emission was observed as the dust devil approached and receded, this being an ultra-low frequency (ULF) electromagnetic emission observed below 50 Hz (also labeled in Figure 3). As described previously [*Houser et al.*, 2003], the emission is observed as a continuous episode of broadband bursty events lasting for over 35 seconds found in two bands between 5–20 Hz and 30–50 Hz. The overall emission intensity for the first 10 seconds remained fairly constant but after that time decreased exponentially by 25 dB over the next 25 seconds in association with the dust devil recession. This emission intensity profile results from the dust devil's transformation from an extended source (∼2π width) to a discrete source (∼1° width near end) as it receded from the truck.

DUST DEVIL PASSAGE

Figure 3. A magnetic spectrogram during the passage of a dust devil.

[23] The ULF magnetic emission is believed to be generated from the cyclonic motion of the charged grains in the dust devil. As charged grains move cyclotrophycally (i.e., horizontal wind velocity proportional to the square root of the pressure drop [*Renno et al.*, 1998]) and vertically in a vortex, the system can be considered a solenoid which is capable of generating a magnetic field. However, the solenoid is not stable, and fluctuates turbulently with the dust devil motion. The solenoid areal dimension variation (ever-changing cross-sectional area) gives rise to a dB/dt, which is detected in the search coil. The observation suggests that the cyclonic fluid motion creates a large-scale magnetic dipole moment, m, associated with the circular solenoid current, m = IA, where I is the total current carried by the grains and A is the dust devil cross-sectional area. This large-scale ULF magnetic moment complements the already known large-scale electric dipole moment of a dust devil [*Freier*, 1960; *Crozier*, 1964; *Farrell et al.*, 1999].

[24] As described previously [*Houser et al.*, 2003], the ULF emission remained roughly constant for the ten second period following interception. However, beyond this time, the ULF emission from the dust devil decreased by ~20 dB

over the next 20 seconds. This roll-off corresponds to $B \sim r^{-2.4}$ implying a radiation pattern between a near and intermediate field. The transmission is consistent with an emission wavelength, λ, greater than the source size, a, and source-to-observer separation distance, r. However, there is a transition from $r < a$ to $r > a$ as the dust devil recedes from the observation point.

[25] As evident in the spectrogram, near 30 seconds (24 seconds after closest approach) the dust devil ULF emission appeared to intensify by ~ 7 dB possibly due to the passage over terrain that enhanced the eolian lifting and subsequent grain charging process either by increasing the number of particles or altering their composition.

[26] While the ULF magnetic observations have been described previously in the initial discovery paper of *Houser et al.* [2003], we review the results here because the emission was observed again a year later during field tests in the Arizona desert. Given the presence of associated DC E-field measurements during this later study, a validity test of the solenoid ULF model of the dust devil can occur.

4.2. Arizona 2001: Base Camp

[27] Between 3−9 June 2001, a large coherent campaign was conducted to study dust devil dynamics in the Arizona desert (~ 5 km southwest of Eloy Az). This study was funded under the auspices of the HEDS/MATADOR program, with field tests designed to demonstrate the integrated measurement concept in preparation for a future flight mission. The team led by U. of Arizona included scientists from GSFC, UC Berkeley, Glenn RC, Ames, JPL, and Optech Inc. A full suite of meteorological, optical, lidar, electric and magnetic instruments were deployed at a fixed station, and a subset of electrostatic and meteorological sensors were mounted on a mobile scientific observing platform (i.e., truck) for pursuit of the dust devils. During the week, dozens of events were observed and we present two representative cases below.

[28] A unique feature of this campaign was the use of a dedicated single data processing system that integrated all the meteorological and electromagnetic data sets. Slow survey-mode data were available, and in addition the system was designed to trigger into a "rapid acquisition mode," sampling electric radios and magnetic search coil antenna at ~ 40 kS/s. Consequently, waveform information was available for specific targets of opportunity. Because of their large data volumes, the camera and lidar systems had their own independent data systems.

[29] Typically, dust devils passed near the camp and remote sensing of the dust devils occurred during these encounters. However, on 7 June, a dust devil fortuitously passed centrally through the camp allowing both remote and in situ electric sensing. The structure was substantial enough to be of consideration and all electrical systems were operational in both slow and high rate modes during the dust devil passage. Manually operated optical systems did

not capture the dust devil and meteorological instrumentation had been moved to the truck (which was not in the area). While associated optical and fluid measurements are not available, this event marked the first time DC-E, AC-E, and AC-B made simultaneous measurements of the same dust devil, with high-rate information (40 kS/s), and consequently, this unique encounter warrants presentation.

[30] Figure 4 displays an overview of the event. The top panel (a) displays the output of the electric field mill (solid black line) and the ULF magnetic activity below 40 Hz (red line) overlaid on the same 600 second (10 min) display. Note that the dust devil approached the base and was capable of being sensed between second of day 52989 and 53054, with direct immersion at second 53031. The field mill was sampled via the nominal slow stream at 10 S/s. However, the ULF magnetic search coil and AC E-field system were sampled at the faster 40 kS/s. Panels (b) and (c) show a 44-second spectrogram during the dust devil immersion period between second 52989 and 53033, with (b) being a spectrogram from the search coil in log format from <1 Hz to 20 kHz and (c) being a spectrogram from an MF E-field radio tuned between 700 and 720 kHz. This radio is basically monitoring a pre-determined quiet portion of the AM radio band. Panel (d) is a spectral slice of the ULF magnetic emission during the dust devil passage at 53028 (14:43:48 PDT).

[31] As suggested by Figure 4a, a most interesting observation is the strong negative excursion of the DC electric field. Note that two dust devils were actually present in the ten minute interval, the first made a closest approach to the base camp at second 52933. However, the second dust devil made a direct pass over the camp, and the associated vertical electric field exceeded -4.3 kV/m. Such large fields saturated the field mill. Because *Freier* [1960] and *Crozier* [1964] measured DC E-fields near ~ 0.6kV/m, such large fields of many kV/m were not anticipated. In fact, the field mill dynamic range was pre-set to be more sensitive assuming that dust devil E-field detection may be difficult. In essence, we embarked on the campaign assuming that fields might be very weak. In fact, the opposite was found to be true with this event exceeding our expectations. Note that these values are larger than any previously reported from a dust devil, and the actual maximum values were not quantified due to instrument saturation.

[32] There are two items to note for the DC E-field observations: First, if this measured vertical E-field persists uniformly throughout the dust devil, the total vertical potential would be nearly ~ 0.8MV, a value similar to those simulated by *Melnik and Parrot* [1998]. While the measured E-fields are 0.1% of terrestrial atmospheric breakdown, they are in fact about $10-20\%$ of the Martian breakdown potential (of ~ 20kV/m [*Farrell et al.*, 1999]). Consequently, a similar charge generation process from a comparable dust devil on Mars would result in electrostatic field values approaching breakdown, again as simulated by *Melnik and*

Figure 4. The electrostatic and electromagnetic activity from a dust devil passage. The top panel overlays measurements from the DC electric field mill with the search coil magnetic antenna. Note that the DC E field gets very large as the dust devil passes, indicating large potential differences within the cyclone. The middle two spectrograms display the search coil and MF radio observations at high resolution. Note that the search coil panel displays activity on a log-frequency scale. The bottom panel is an individual spectrum from the search coil during the dust devil passage at second 53028.
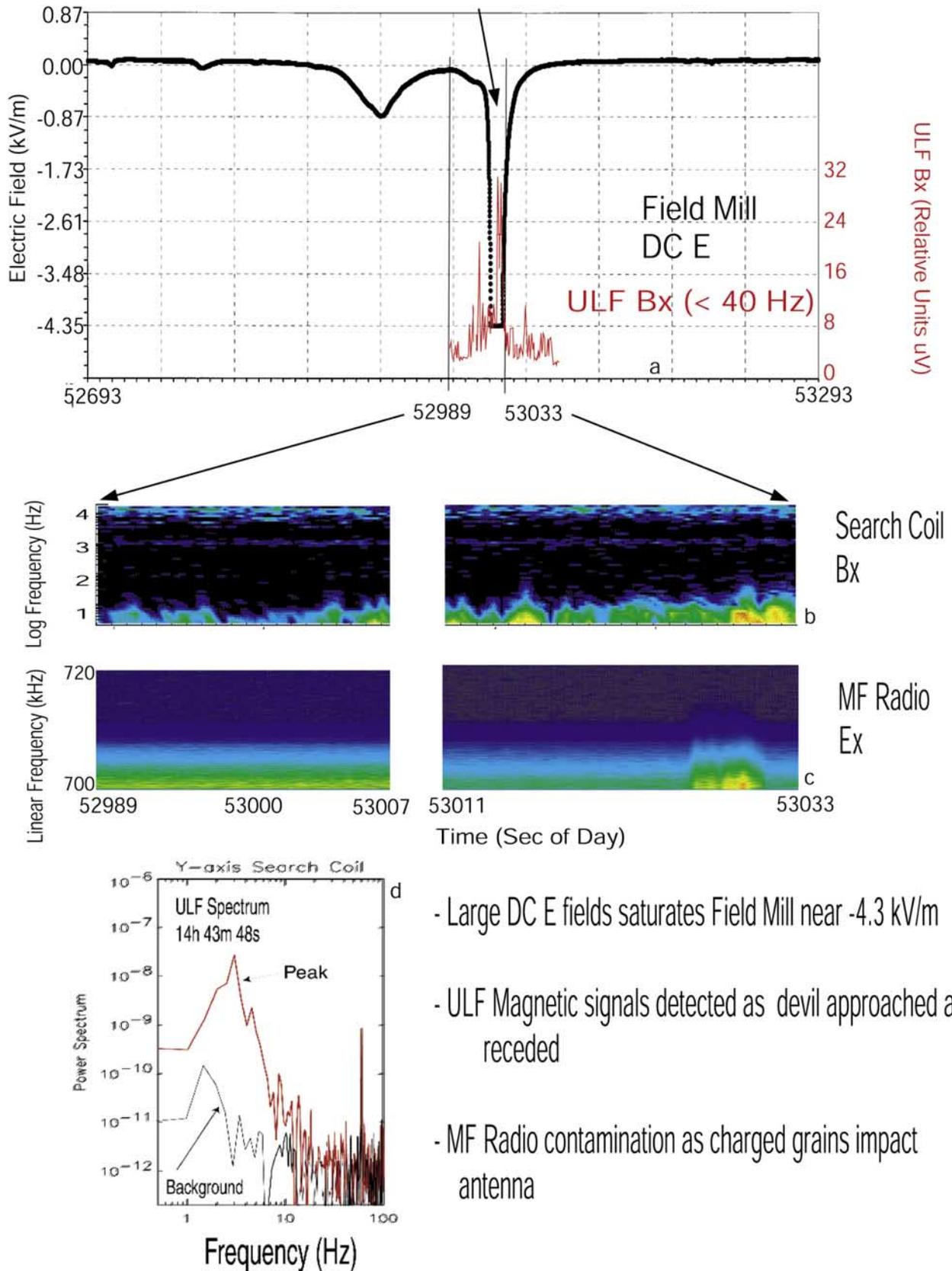
Figure 4.

Parrot [1998]. Second, the upward (skyward) direction of the electric field, based on the negative values in Figure 4a, is consistent with the dust devil possessing an inverted electric dipole moment, like that displayed in Figure 2, with lighter negative grains being mass stratified to the dust devil top. *Crozier*'s [1964] observations indicated a similar situation in the dust devil.

[33] Well away from the dust devil, the fair-weather electric field at ground is detected as a slight positive displacement away from zero (e.g., at end of plot, second 53293, E-field is ∼+70 V/m). This electric field, as expected, is nadir pointing.

[34] As indicated in Figures 4a, 4b, and 4d, a ULF magnetic emission was again detected from the dust devil (as in July 2000), this occurring between 1–10 Hz. As Figure 4a indicates, the emission was detected for about 70 seconds, with peak values occurring simultaneously with the maximum values obtained by the DC E field mill. The spectrogram in Figure 4b consists of consecutive FFT analysis of the search coil magnetic fields sampled at 40 kS/s and indicates a steadily rising emission level at and below 10 Hz, peaking in a "double maximum" near second 53031 and 53032. The emission also had its largest bandwidth at this time, with enhanced emission levels extending nearly 100 Hz. Note that the ordinate in Figure 4b is the log of the frequency. Figure 4d is a spectral slice from near second 53028, indicating the enhanced ULF magnetic emission levels of nearly 100 times background levels in the vicinity of the dust devil. A clear monochromatic spike at 60 Hz is also obvious in the spectrum. Visible from the site were high-tension power lines that are a known source of 60 Hz emission and their location over a sandy surface (i.e., insulator) would allow efficient propagation of radiation to the base camp site [*Farrell et al.*, 1998].

[35] Figure 4c shows the RF emission levels (700–720 kHz) from an exposed electric whip antenna. Note that the signal levels display a broadband intensification for a 5 second period near second 53026–53032. This broadband noise is associated with the discharge of charged grains to the antenna, which gives rise to a voltage spike $V = Q/C$ where C is the antenna capacitance [*Farrell et al.*, 2000]. Such spikes, when spectrally analyzed, give rise to a broadband signal that is detectable in the radio (similar spikes observed in Figure 3 at second 5 to 6). A near-continuous series of these discharges gives rise to a quasi-continuous broadbanded signal in the RF. This emission, which is generated in situ, indicates the exact times the charged dust devil passed over the camp. This observation is indicative of tribocharging at the individual grain level. Assuming a speed of 1–3 m/sec, and a 5 second emission duration, a dust devil diameter of 10 m is inferred. As indicated in Figures 4a and 4b, both the dust devil's DC E and ULF B signatures were detected about 30 seconds prior to the actual dust devil interception (initial detections near second 52990) suggesting that the dust devil can be remote sensed about 30–90 m before its actual incidence.

[36] Given the E-field values, an estimate of the charge density can be derived assuming that the dust devil is an electric dipole with negative grains at the top and positive charges at the bottom. This approach was applied by *Crozier* [1964] and *Farrell et al.* [1999] in estimating charge density of the dust devils. In a region where the
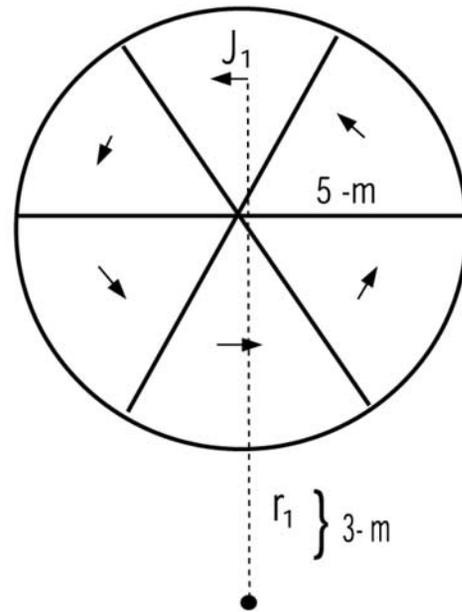

Figure 5. The magnetic field determination based on dividing the cyclonic dust devil into six pieces and calculating their contribution to the total magnetic field via $B \sim (4\pi)^{-1}\mu_o\Sigma(\mathbf{J_i}x\mathbf{r_i})|\mathbf{r_i}|^{-3}\Delta V \sim (4\pi(25.6 \text{ m}^2))^{-1}\mu_o env$ ΔV for the dimensions shown. Given a measurement of B and an estimate of particle velocity and volume, an approximate quantification of charge density, n, can be obtained.

dust devil-to-observer distance is comparable to the dust devil height, the electric field can be approximated as $E = 2Qh/4\pi\varepsilon_o r^3 \sim Q/2\pi\varepsilon_o r^2$ where $-Q$ charge congregates at the dust devil top and $+Q$ charge congregates at the dust devil base. Assuming this charge is uniformly distributed over $^1/_2$ the dust devil volume ($-Q$ over top half; $+Q$ over bottom half) a charge density of

$$n \sim 4\pi\varepsilon_o r^2 E/V \qquad (1)$$

is obtained using a volume of V/2. The field mill saturates at E = 4.3 kV/m at a distance of r ∼ 50 m from the dust devil interception. Inserting these values into equation (1) yields an estimate of the density n ∼ 10^6 el/cc. This value is similar to that derived in the *Crozier* [1964] case.

[37] This density can be compared to that derived from the corresponding ULF magnetic field measurements. In this case we treat the dust devil as a solenoid ULF emission source (as suggested by Figure 4a of *Houser et al.* [2003]). Specifically, below 40 Hz, the ratio of output voltage from the search coil preamp to the measured magnetic field is 80 μV/nT. The measured magnetic field just outside the dust devil is ∼8 μV (see Figure 4a), corresponding to a B ∼ 0.1 nT. In order to estimate the charge density of the dust devil, the Biot-Savart law was applied by dividing the dust devil into 6 equal areal sections and summing the contribution to the magnetic field on a section-by-section basis (Figure 5). This method assumes a constant current density, grain speed, and dust devil volume (i.e., static/near field

calculation). The charged particle density based on this approach is approximately

$$n \sim 4\pi(25.6 \text{ m}^2)B/\mu_o ev\Delta V \qquad (2)$$

where v is the flow speed of the dust devil and ΔV is the volume of a dust devil slice (1/6 the total dust devil volume of $\pi a^2 h$, a being the radius and h the height). Applying equation (1) with a dust devil wind rotational velocity of $\sim$30 m/sec and a 1/6 volume element of 1300 m^3 we obtain a density of 5×10^6 el/cm^3 which is on the same order as that determined by the electric field system. The ULF response is associate with a dB/dt from the fluctuation changing volume of the dust devil, with a solenoid cross-section that is in continual variation.

[38] It is concluded that the magnetic solenoid model of the dust devil obtains a consistent result with the electrostatic capacitor model of the dust devil, giving density estimates on the same order. The magnetic emissions are a by-product of the electrostatic tribocharging process.

4.3. Arizona 2001: Truck Observations

[39] As with the Nevada 2000 campaign, a mobile platform (i.e., truck) was also available in Arizona to track and intercept dust devils. The truck was outfitted with a meteorological station consisting of pressure, temperature and wind velocity sensors and an electrometer to measure relative electric potential. These instruments were located on masts whose bases were anchored in the bed of the truck. In Nevada, the truck could travel anywhere on a flat, 8 square mile playa driving directly into active dust devils relatively easily. In Arizona, the truck had limited 2-D capability and was confined to roads and only few fields. Thus there were fewer direct interceptions in this later campaign.

[40] Despite this difficulty, a direct truck interception with a small dust devil occurred in an accessible field adjacent to the base camp on 6 June at 1:18 PM. Figures 6, 7, and 8 show the observations and configuration, respectively, during the truck passage through the dust devil of modest size. Figure 6 shows the (a) wind speed, (b) wind direction, (c) temperature, (d) pressure difference from ambient, and (e) electrostatic potential. Figure 7 schematically illustrates the encounter geometry while Figure 8 is a photo of the dust devil.

[41] The following describes the generation of Figures 6 and 7: The truck drove through the dust devil, then stopped in its path. In Figure 6b, the second change in wind direction thus corresponds to the dust devil passage over the stationary truck. The wind velocity, Figure 6a, corresponds to the wind data after correcting for the motion of the truck, determined from a GPS transceiver, and for the whole-body motion of the dust devil. The latter was estimated from the prevailing winds before and after the dust devil passage, from interpolating multiple observations of the same dust devil, and from written log entries. The erratic motion of the dust devil makes such an estimation only approximate. The dust devil/truck encounter appears to go very close to the eye of the dust devil, as indicated by the nearly 180 degree direction change and the corresponding drop to near-zero velocity. Much like the observations of Martian dust devils by Viking [*Ryan and Lucich*, 1983], these terrestrial dust devils are found to possess "hot cores"

with temperatures steadily rising and ultimately peaking in the dust devil center (Figure 6c). As with the Mars Pathfinder meteorology results [*Schofield et al.*, 1997; *Murphy and Nelli*, 2002], a small but detectable pressure decrease (1–2 mb) occurs in the dust devil center. The observations of thermal and pressure gradients suggest the dust devil is a miniconvective system, with fluid cyclonic motion (winds) ultimately driven by near-ground thermal energy. The lower pressure and increased temperature in the dust devil center results in ascending fluid elements [*Renno et al.*, 1998] that also carry lighter grains upward. Finally, Figure 6e indicates a substantial change in potential from ambient values during the dust devil passage, indicating a source of dust devil related atmospheric electricity.

[42] It is interesting to note that the dust devil electric potential and local pressure difference are strongly correlated, with two large local maxima in negative potential correlated with local minima in pressure. However, the pressure difference from ambient is so slight that there is only a small change in ambient Paschen breakdown voltage (which scales directly with pressure). Thus the measured potential changes are not considered associated with changes in the atmospheric gas density. For example, the Paschen breakdown potential is typically $\sim$20000 V at a few centimeters for the terrestrial atmosphere at ground level [*Uman*, 1969]. This value scales directly with ambient pressure, and the few millibar change in pressure observed within the dust devil would correspond to only a 20–60 V potential variation. However, as indicated in Figure 6e, the ambient potential changed by orders of magnitude within the dust devil interior over ambient levels measured outside the dust devil. As earlier, we conclude that the potential results from the charged grains and the formation of coherent charge centers in the dust devil, rather than a change in the atmospheric density and Paschen gas breakdown characteristics. While there is a relationship between P and potential, ϕ, this relationship does not appear to be direct.

5. Conclusions

[43] Many events were detected during the 2000 and 2001 campaigns and here we attempt to show some representative cases that illustrate the fluid and electrical properties of these interesting minicyclones. These cases also represent times when the desired sensors were operational, which did not always occur during the most fortuitous events. Thus we present cases where both human and natural factors were maximized. Despite this, the data sets represent a coherent, multisensor investigation of dust devils with some rather interesting and new conclusions:

[44] 1. The electric fields within about 50 m of some of the larger dust devils saturated at 4 kV/m, field values larger than we anticipated. The electric field values measured are consistent with assuming the dust devil is generating charge centers of opposite polarity at the dust devil base and dust devil top, creating a large-scale macroscopic electric dipole moment.

[45] 2. A magnetic ULF emission was sensed from the dust devil and had intensities consistent with radiation from cyclostrophic motion of charged grains. In this case, the dust devil has a macroscopic magnetic dipole moment similar to that expected from a solenoid-shaped structure.
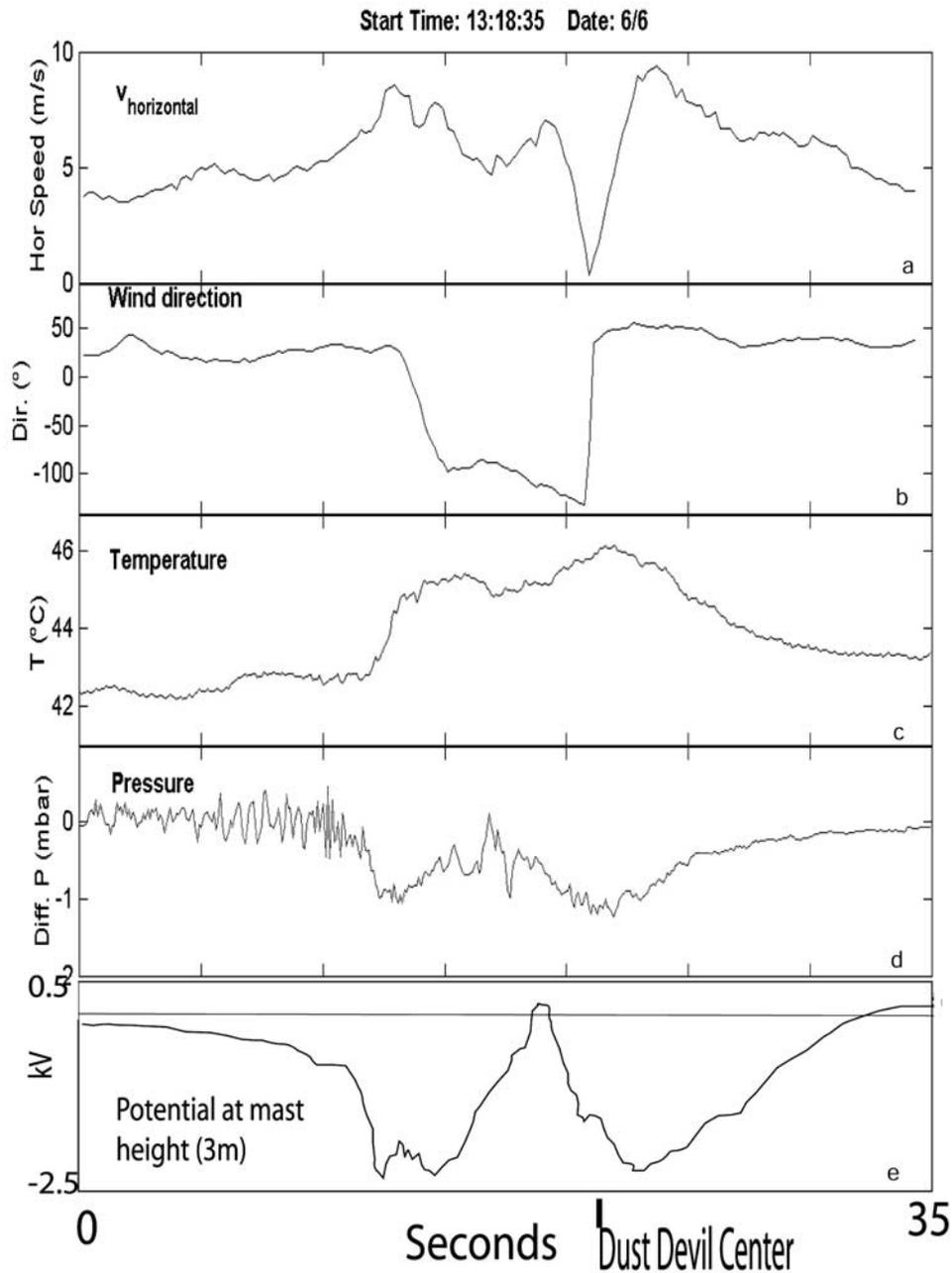
Figure 6. Wind speed, direction, temperature, pressure and relative potential during a dust devil passage.

Further, the charge density required for the magnetic intensities from the large-scale magnetic dipole moment is consistent with that associated with the large-scale electric dipole moment (equations (1) and (2) consistent).

[46] 3. As the dust devil passed over the sensor, a series of broadband RF spikes are commonly detected as the charged grains impact with either a bare antenna or exposed conducting/capacitive surface of the sensor. On any exposed electric system, this would appear as noisy "static" and lead to RF contamination.

[47] 4. A correlation between local electrostatic potential and pressure in the dust devil is observed, but their relationship is believed to be indirect, with the dust devil potential differences far exceeding that anticipated from

changes in the local atmospheric potential resulting from pressure differences.

[48] The MATADOR study can place some perspective on the dust devil energy budget. The energy partition of the dust devil is itemized in Table 1. Specifically, the dust devil's thermal energy, based on an assumed dust devil pressure variation from ambient of a few mb (like those observed on the truck, Figure 6), is $\sim 10^2$ J/m^3. The dust devil's kinetic energy is in excess of 0.1 J/m^3, assuming values at or above the following: Grain density of >100/cm^3, grains speeds of >10 m/sec and average dust devil grain size of >10 μm in the column. Conversely, the electrostatic energy in the dust devil, defined by $\varepsilon_o E^2$ (using field values measured directly by MATADOR) is approximately
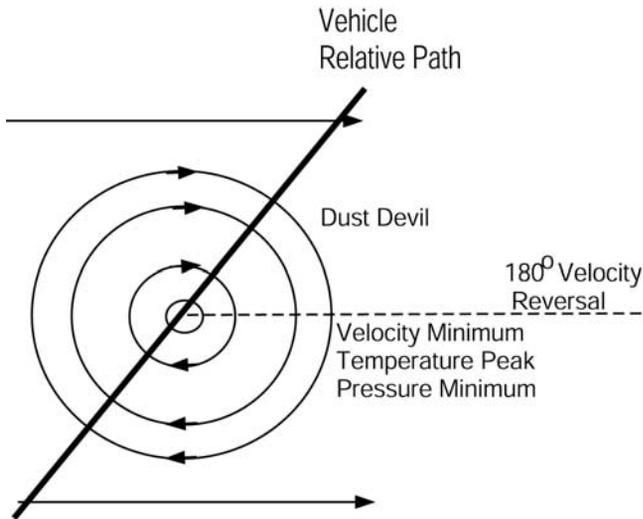
Figure 7. An illustration of the truck passage through the dust devil, approximately corresponding to the observations in Figure 6. The truck travels from the bottom to the top of the figure.

Table 1. Energy Density Partition of a Dust Devil

Energy	Value
Thermal energy ($3/2 \, \Delta P$)	100 J/m^3
Kinetic energy ($\rho m v^2$)	>0.1 J/m^3
Electric energy ($\varepsilon E^2/2$)	>10^{-4} J/m^3
ULF magnetic energy ($B^2/2\mu_o$)	10^{-12} J/m^3

10^{-4} J/m^3. The electric energy is calculated using the known values at saturation in Figure 4, and thus is considered an underestimate. The calculations suggest a conversion of thermal-to-electrostatic energy of 10^{-5} to 10^{-6}. The conversion of thermal-to-electrostatic energy in a terrestrial thunderstorm is $\sim10^{-2}$ [*Volland*, 1984], suggesting that thunderstorm inductive processes are more efficient than triboelectric processes at electrostatic energy generation. The dust devil electromagnetic energy in the ULF, $\sim B^2/\mu_o$ (again using MATADOR measurements) is on the order of a 10^{-12} J/m^3, suggesting that a very small fraction of the dust devil thermal energy converts to ULF EM emissions. The ULF emission is a by-product of the larger electrostatic processes. We conclude that the dust devil is a moderately efficient triboelectric generator that feeds charge centers, but

a rather inefficient EM emitter in the ULF band (inefficient in converting fluctuations in areal size into low frequency EM radiation).

[49] Can we compare terrestrial and Martian dust devils? As suggested by Figure 6, terrestrial dust devils have hot cores, cyclonic winds and pressure decreases that almost exactly mirror their Martian counterparts [*Ryan and Lucich*, 1983; *Murphy and Nelli*, 2002]. These fluid forces give rise to grain mass stratification for dust devils on both planets. If a mass-dependent contact electrification process is also present, the initially mixing but lofted grains will become charge stratified within the dust cloud. Our observations of a large vertical electric field confirm the presence of separate charge centers in the dust devil, consistent with the *Melnik and Parrot* [1998] picture. Since contact electrification is not unique to any one of the two planets, a similar electrical phenomenon is anticipated for Mars, as long and the Martian grains have variable compositions and sizes. As described by *Farrell et al.* [2003], the primary electrical difference between the two planets is the near-surface atmospheric conductivity, which is anticipated to be a factor of 100 times greater on Mars as compared to the Earth (due to the lower ambient neutral density). The primary effect of this higher conductivity is to create a larger dissipation "return" current (σE) to the Martian atmosphere, this being a separate current pathway that draws charge away from the primary triboelectric currents. The effect does not reduce the overall electric field, but will make the Martian dust devil charge-up process slower as compared to their terrestrial counterparts [*Farrell et al.*, 2003].
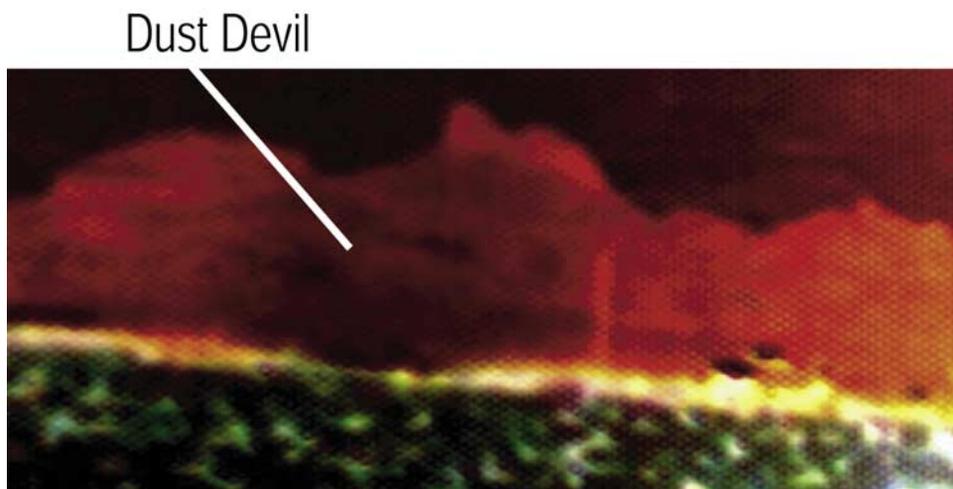

Figure 8. A false-color image of a dust devil, the dark shadow, against the backdrop of lighter, distant mountains. A truck with meteorology equipment is located just to the side of the dust devil, and is about to make a direct interception with the dust devil. The associated electro-meteorology data are displayed in Figure 6.

[50] While triboelectric Martian dust storm charging is not as efficient per volume as terrestrial thunderstorm inductive processes, the global atmospheric electric content of the two planets may actually be comparable simply by the shear volume associated with the larger Martian dust storms. The electrostatic energy of a single nominal thundercloud (of volume of $\sim 10^{11}$ m^3) is $\sim 10^{11}$ J [*Volland*, 1984] corresponding to an energy density of ~ 1 J/m^3. This density value is a factor of 10000 times greater than that in a dust cloud. Given that there are approximately 2000 thunderstorms ongoing over the entire Earth, the volume of terrestrial atmosphere in thunderclouds is $\sim 10^{14}$ m^3, making the global atmospheric electric content on Earth at any given time about 10^{14}–10^{15} J.

[51] If we assume that Martian dust clouds contain similar electrostatic energy densities as measured in the Arizona tests ($>10^{-4}$ J/m^3), then a Martian dust cloud extending $\frac{1}{2}$ the globe and 10 km in height (10^{18} m^3) would have a total global atmospheric electric content of nearly 10^{14} J, a total global value comparable to that of Earth's. The factor of 10000 decrease in efficiency of tribocharging on Mars compared to inductive processes on Earth is offset by the factor of 10000 volume increase in Martian storm size.

[52] This calculation assumes a similar electric energy density as derived from the field tests. It also assumes a large extended dust cloud where nearly all grains have undergone mixing/collisions before moving into the non-mixing regions. Further, we assume all grains retain their charge in the nonmixing regions. The calculation is just one possible scenario for the distribution of electric energy on the planet and is not a unique solution. There are other ways to distribute the global atmospheric electric energy [e.g., see *Farrell and Desch*, 2001].

[53] A primary objective of the MATADOR study was to determine the possible hazards associated with charged dust devils on Mars. If the calculations above prove to be true, a primary process on Mars, as it is on Earth, is the dissipation of the electric energy back into the atmosphere and ground. Electric energy does not persist, but "relaxes" back into the atmosphere either via slow leaking of charge into the atmosphere (corona-like current) or impulsive breakdown (lightning). The quantity and form of Martian dissipative processes is speculative at this point, but for a large electric atmospheric content, such processes must exist, since charge relaxation is a fundamental physical process (i.e., objects do not store charge indefinitely but leak charge into their surroundings on timescales of ε_o/σ, σ being the object conductivity). From a meteorological perspective, it is the dissipative effects associated with stored electric energy that give rise to hazards. For example, if too much electric energy develops locally, electrical discharge will occur, dissipating energy via arcing into atmospheric heating, RF radiation, etc. Even if the electric energy levels do not approach breakdown, the ε_o/σ relaxation of dust charge back into the atmosphere increases the near-surface electron content, which then affects dust adhesion, and sensitive electric equipment. Unlike the Earth, an end-to-end, traceable understanding of the Martian atmospheric electricity generation, storage, and dissipation currently does not exist. This understanding will ultimately lead to a prediction of any electrical hazards.

Given that sensitive hardware and possibly humans may have to survive a long lasting global Martian storm, it would be prudent to further pursue these basic atmospheric electrical measurements.

[54] The hazards of an electrified dusty atmosphere were discussed in the recent *National Research Council* [2002] report. In that report, electric hazards from a dusty atmosphere are identified as a problem that requires added design considerations in any human or robotic mission. In that report, the science committee concluded that tricharging will occur in dust devils, but contend that equal amounts of positive and negative charge will be contained in any given dust devil volume element, making the dust devil quasi-neutral (i.e., no large intra-devil potentials will develop). In contrast, we conclude here that the dust devil cannot be quasi-neutral, and must consist of well-separated quasi-vertically aligned charge centers in order to account for the observed large-scale vertical electric fields detectable well outside the devil and which smoothly vary to >4 kV/m within the structure itself (Figure 4). The dust devil behaves as a natural electric generator, tribo-charging [*Ette*, 1971; *Desch and Cuzzi*, 2000] and separating grains on the basis of their mass, generating voltages possibly in excess of 0.5 MV. Thus we expand upon the NRC's conclusions and suggest that dust devils are very electrically energetic and worthy of further study both on Earth as an analog to Mars, and on Mars itself.

References

Ashcroft, N. W., and N. D. Mermin (1976), *Solid State Physics*, Holt, Rinehart, and Winston, Forth Worth, Tex.

Bagnold, R. A. (1941), *The Physics of Blown Sand and Desert Dunes*, Methuen, New York.

Crozier, W. D. (1964), The electric field of a New Mexico dust devil, *J. Geophys. Res.*, 69, 5427.

Desch, S. J., and J. N. Cuzzi (2000), The generation of lightning in the solar nebula, *Icarus*, 143, 87.

Eden, H. F., and B. Vonnegut (1973), Electrical breakdown caused by dust motion in low pressure atmospheres: Considerations for Mars, *Science*, 180, 962.

Ette, A. I. I. (1971), The effect of Hermattian dust on atmosphere electric parameters, *J. Atmos. Terr. Phys.*, 33, 295.

Farrell, W. M., and M. D. Desch (2001), Is there a Martian atmospheric electric circuit?, *J. Geophys. Res.*, 106, 7591.

Farrell, W. M., M. D. Desch, and J. G. Houser (1998), Modification of the upper atmosphere over power lines: A geological effect, *J. Geophys. Res.*, 103, 11,573.

Farrell, W. M., M. L. Kaiser, M. D. Desch, J. G. Houser, S. A. Cummer, D. M. Wilt, and G. A. Landis (1999), Detecting electrical activity from Martian dust storms, *J. Geophys. Res.*, 104, 3795.

Farrell, W. M., M. D. Desch, M. L. Kaiser, J. Houser, G. A. Landis, and D. M. Wilt (2000), Radio and optical detection of Martian dust storm discharges, *Acta Astronaut.*, 46, 25.

Farrell, W. M., G. T. Delory, S. A. Cummer, and J. R. Marshall (2003), A simple electrodynamic model of a dust devil, *Geophys. Res. Lett.*, 30(20), 2050, doi:10.1029/2003GL017606.

Freier, G. D. (1960), The electric field of a large dust devil, *J. Geophys. Res.*, 65, 3504.

Gierasch, P. J. (1974), Martian dust storms, *Rev. Geophys.*, 12, 730.

Gierasch, P. J., and R. M. Goody (1973), A model of a Martian great dust storm, *J. Atmos. Sci.*, 30, 169.

Greeley, R., R. Leach, B. R. White, J. D. Iversen, and J. B. Pollack (1980), Threshold wind speeds for sand on Mars: Wind tunnel simulations, *Geophys. Res. Lett.*, 7, 121.

Greeley, R., B. R. White, R. Leach, R. Leonard, J. Pollack, and J. D. Iversen (1981), Dust storms on Mars: Considerations and simulations, *Geophys. Soc. Am. Spec. Pap.*, 186, 101.

Greeley, R., N. Lancaster, S. Lee, and P. Thomas (1992), Martian eolian processes, sediments and features, in *Mars*, edited by H. H. Kieffer et al., pp. 730–766, Univ. of Ariz. Press, Tucson.

Houser, J. G., W. M. Farrell, and S. M. Metzger (2003), ULF and ELF magnetic activity from a terrestrial dust devil, *Geophys. Res. Lett.*, *30*(1), 1027, doi:10.1029/2001GL014144.

Iversen, J. D. (1976), Wind-blown dust on Earth, Mars, and Venus, *J. Atmos. Sci.*, *33*, 2425.

Jayaratne, E. R. (1991), Charge separation during the impact of sand on ice and its relevance to theories of thunderstorm electrification, *Atmos. Res.*, *26*, 407.

Marshall, J. G. (1994), Particle Dispersion Experiment (PDE): Preliminary results from the USML-1 glovebox, *NASA Conf. Publ., NASA CP-3272*, 717.

Melnik, O., and M. Parrot (1998), Electrostatic discharge in Martian dust storms, *J. Geophys. Res.*, *103*, 29,107.

Mills, A. A. (1977), Dust cloud and frictional generation of glow discharges on Mars, *Nature*, *268*, 614.

Murphy, J. R., and S. Nelli (2002), Mars Pathfinder convective vortices: Frequency of occurrence, *Geophys. Res. Lett.*, *29*(23), 2103, doi:10.1029/2002GL015214.

National Research Council (2002), *Safe on Mars: Precursor Measurements Necessary to Support Human Operations on the Martian Surface*, Natl. Acad. Press, Washington, D. C.

Renno, N. O., M. L. Burkett, and M. P. Larkin (1998), A simple thermodynamic theory of dust devils, *J. Atmos. Sci.*, *55*, 3244.

Ryan, J. A., and R. D. Lucich (1983), Possible dust devils, vortices on Mars, *J. Geophys. Res.*, *88*, 11,005.

Schofield, J. T., J. R. Barnes, D. Crisp, R. M. Haberle, S. Larsen, J. A. Magalhães, J. R. Murphy, A. Seiff, and G. Wilson (1997), The Mars Pathfinder atmospheric structure investigation/meteorology (ASI/MET) experiment, *Science*, *273*, 1752.

Smith, P. H., and M. Lemmon (1999), Opacity of the Martian atmosphere measured by the imager on Mars Pathfinder, *J. Geophys. Res.*, *104*, 8975.

Uman, M. A. (1969), *Lightning*, McGraw-Hill, New York.

Volland, H. (1984), *Atmospheric Electrodynamics*, Springer-Verlag, New York.

————————————

D. Catling, Department of Atmospheric Sciences, University of Washington, Box 351640, Seattle, WA 98195-1640, USA.

S. A. Cummer, Department of Computer and Electrical Engineering, Duke University, Durham, NC 27706, USA.

G. T. Delory, Space Science Laboratory, University of California, Berkeley, CA 94720, USA.

M. D. Desch, W. M. Farrell, and J. G. Houser, NASA Goddard Space Flight Center, Mail Code 695, Greenbelt, MD 20771, USA. (william.farrell@gsfc.nasa.gov)

M. Hecht and D. M. Tratt, Jet Propulsion Laboratory, 4800 Oak Grove Drive, Pasadena, CA 91109-8099, USA.

G. B. Hillard and B. Johnson, NASA Glenn Research Center, Lewis Field, 21000 Brookpark Road, Cleveland, OH 44135, USA.

J. R. Marshall, SETI Institute, 2035 Landings Drive, Mountain View, CA 94043, USA.

N. Renno, Atmospheric, Oceanic and Space Sciences, University of Michigan, Ann Arbor, MI 48109, USA.

P. H. Smith, Lunar and Planetary Laboratory, University of Arizona, Tucson, AZ 85721, USA.